

Supporting Information

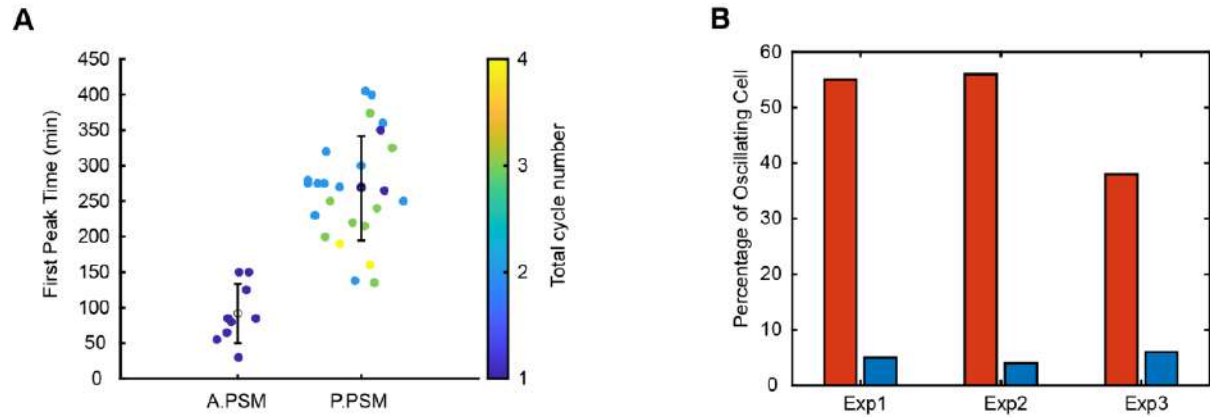


Figure S1: Oscillation dynamics of isolated cells from different regions of the zebrafish embryo tail and the influence of surface coatings on the percentage of oscillating cells. (A) Isolated cells were obtained from different cutting positions along the zebrafish embryo tail: anterior presomitic mesoderm (A.PSM) and posterior presomitic mesoderm (P.PSM). The violin plot of the first peak time indicates that oscillating cells isolated from the A.PSM expressed their peaks earlier than those from the P.PSM (N = 9 for A.PSM and N = 26 for P.PSM). This suggests that the oscillation dynamics of individual cells may vary depending on their original location within the presomitic mesoderm.

(B) Comparison of the percentage of oscillating cells cultured on Pluronic-coated glass (red) and Matrigel-coated glass surfaces (blue) across three independent experiments. The percentage of oscillating cells on Pluronic-coated glass was consistently around 45%, while on Matrigel-coated glass, it was approximately 5%. The number of tracked cells for each condition and experiment is as follows:

- Exp1: N = 31 for Pluronic-coated glass and N = 40 for Matrigel-coated glass
- Exp2: N = 62 for Pluronic-coated glass and N = 48 for Matrigel-coated glass
- Exp3: N = 29 for Pluronic-coated glass and N = 71 for Matrigel-coated glass

These findings demonstrate that the surface coating significantly influences the proportion of isolated cells that exhibit oscillatory behavior, with Pluronic-coated glass promoting a higher percentage of oscillating cells compared to Matrigel-coated glass.

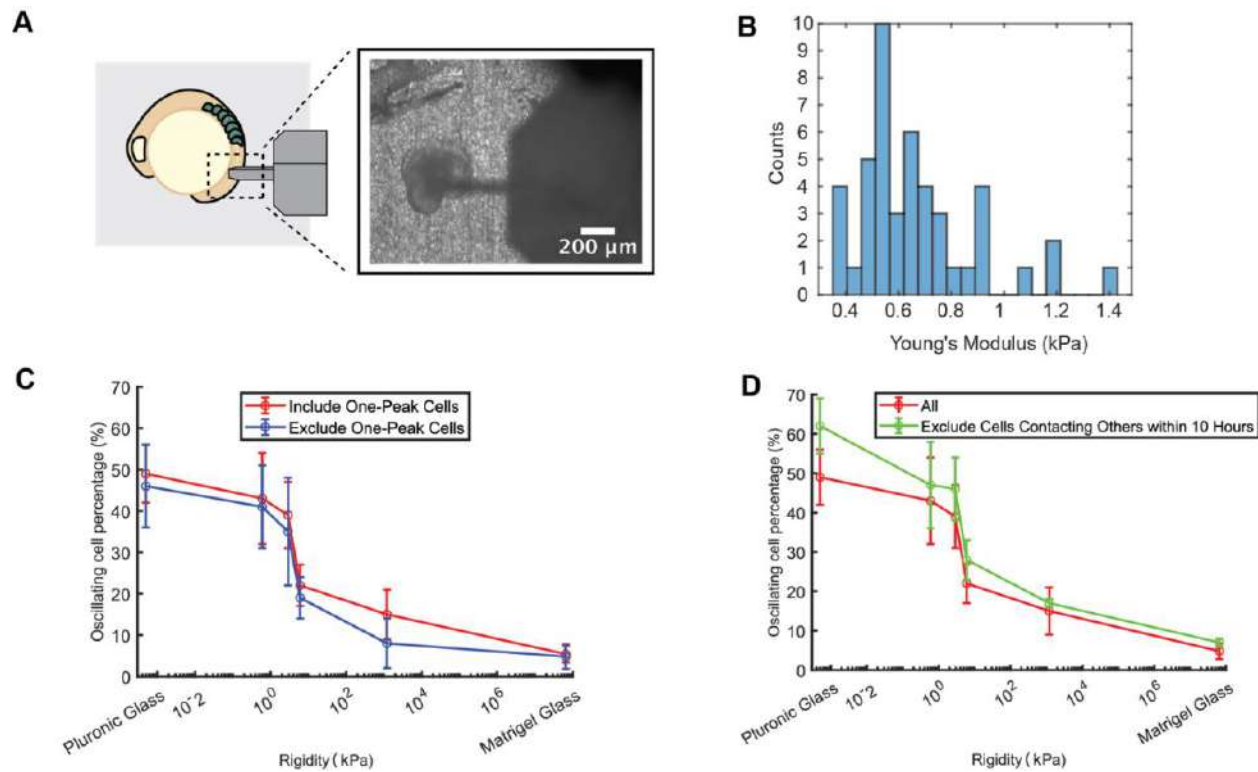


Figure S2: Measurement of posterior presomitic mesoderm (P.PSM) rigidity using an atomic force microscope and the influence of cell selection criteria on the percentage of oscillating cells. (A) Rigidity measurement of the P.PSM using an atomic force microscope (AFM). The AFM tip was positioned on the P.PSM, and a total of 46 data points were collected within a $0.5 \mu\text{m} \times 0.5 \mu\text{m}$ square along the P.PSM. (B) Young's modulus of the P.PSM was determined to be 0.67 ± 0.04 kPa (mean \pm standard error). This quantitative assessment of tissue rigidity provides a reference point for understanding the mechanical environment experienced by cells within the P.PSM. (C) The percentage of oscillating cells, after excluding cells exhibiting only a single peak, still displayed a switch-like behavior as a function of surface rigidity. This suggests that the observed trend in the percentage of oscillating cells is robust and not significantly influenced by the inclusion or exclusion of single-peak cells in the analysis.

(D) The percentage of oscillating cells, after excluding cells that contacted other cells within 10 hours, also maintained the switch-like behavior. This indicates that the observed trend in the percentage of oscillating cells is not primarily driven by cell-cell contact events occurring within the first 10 hours of the experiment.

A

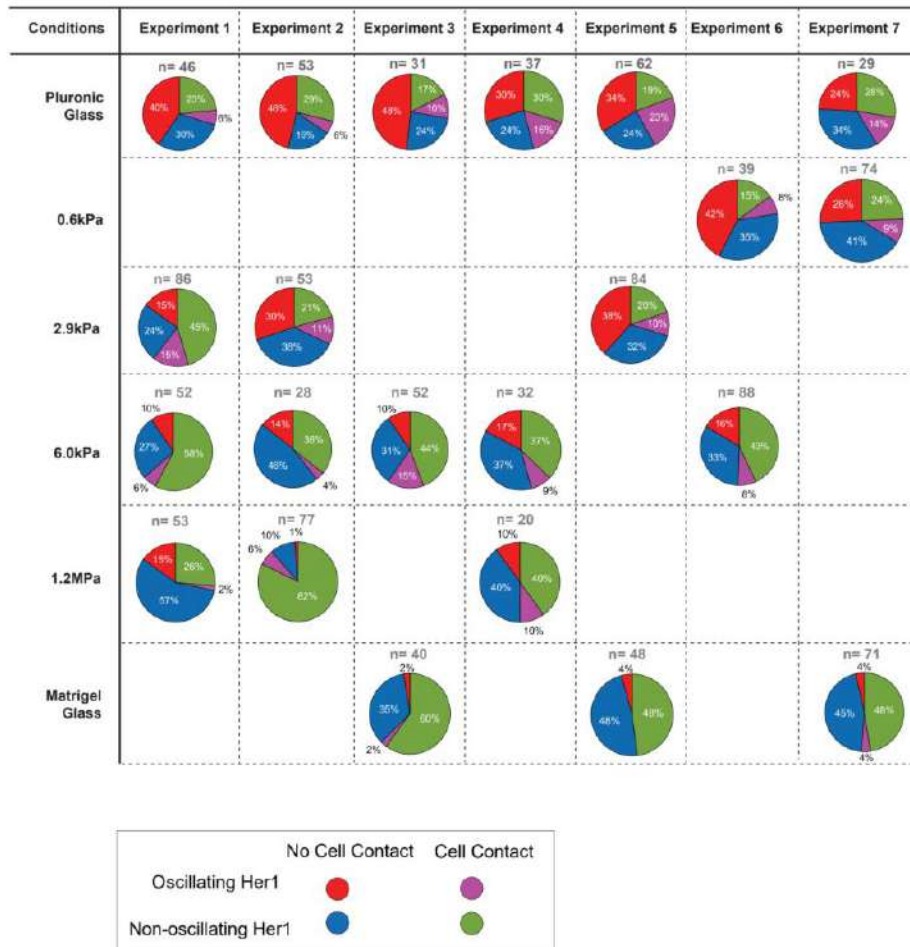


Figure S3: Proportions of oscillating and non-oscillating cells, and their contact status, across different surface conditions. (A) Pie charts represent the distribution of cell behaviors and contact status for each dataset and surface conditions. All cells included in the analysis were initially isolated in the first frame and could be tracked for 10 hours. The following categories are represented:

- Red: Oscillating cells that remained isolated for the entire 10-hour period
- Blue: Non-oscillating cells that remained isolated for the entire 10-hour period
- Pink: Oscillating cells that contacted other cells after the first frame and within the 10-hour period
- Green: Non-oscillating cells that contacted other cells after the first frame and within the 10-hour period

On rigid micropost surfaces (1.2 MPa) and Matrigel-coated glass, a larger proportion of cells contacted other cells within the 10-hour observation period compared to softer micropost surfaces (0.6 kPa and 2.9 kPa) and Pluronic-coated glass. This suggests that surface rigidity and coating properties may influence cell migration and cell-cell interactions, in addition to their effects on oscillatory behavior.

The pie charts provide a comprehensive overview of the distribution of cell behaviors and contact status across the different experimental conditions, allowing for a direct comparison of the relative proportions of each category. This visualization complements the main figures by offering additional insights into the interplay between surface properties, cell oscillations, and cell-cell interactions.

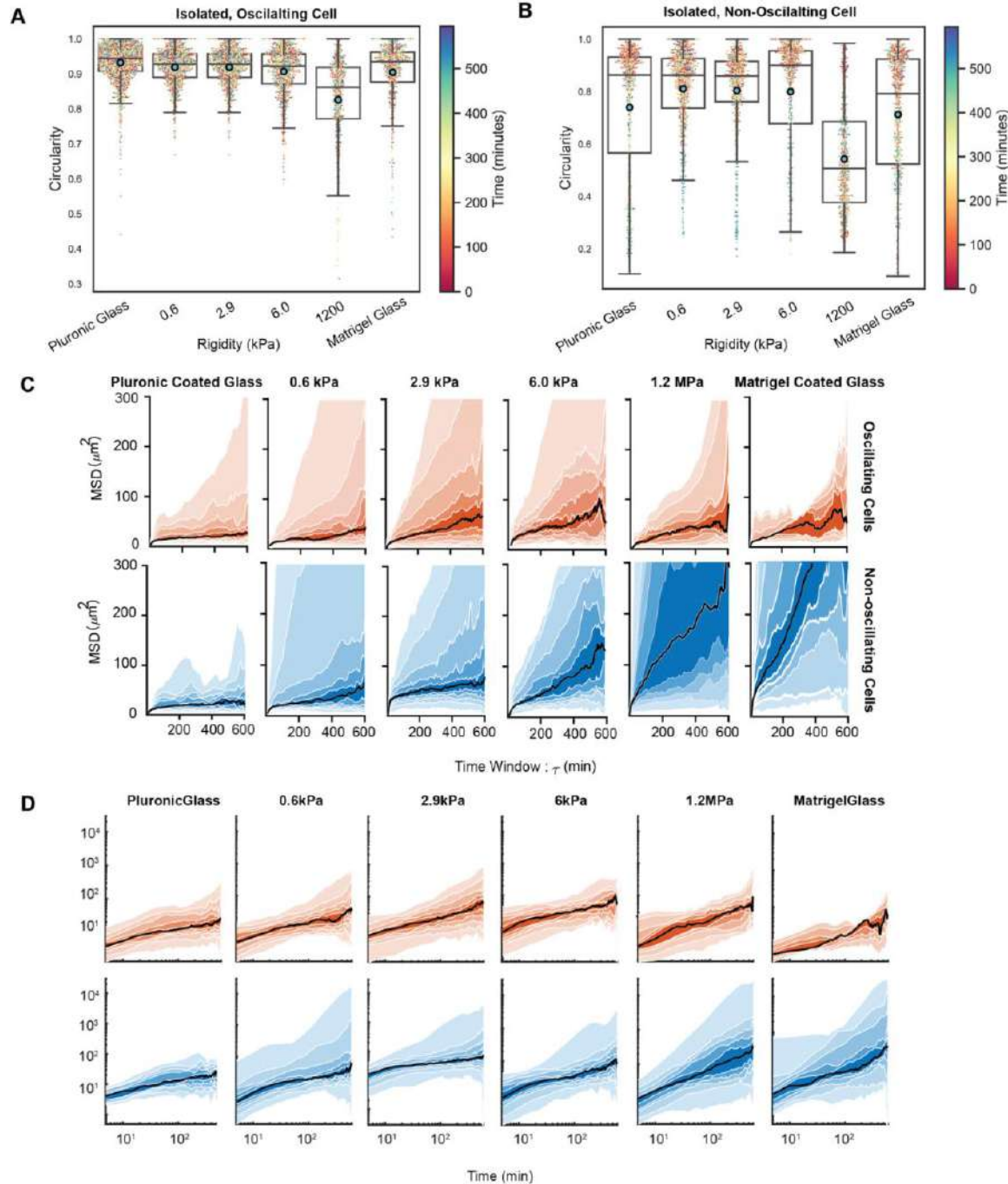


Figure S4: Circularity, windowed mean squared displacement (MSD), and traction force analysis of oscillating and non-oscillating cells on surfaces of varying rigidities. (A) The circularity of isolated oscillating cells on surfaces of varying rigidities. Oscillating cells display higher and more consistent circularity values on soft micropost arrays (0.6 kPa and 2.9 kPa) compared to rigid micropost arrays (1.2 MPa) and Matrigel-coated glass. (B) The circularity of isolated non-oscillating cells on surfaces of varying rigidities. Non-oscillating cells exhibit a wide range of circularity values on rigid micropost arrays (1.2 MPa) and Matrigel-coated glass, suggesting more variable cell morphologies on these surfaces. (C) Windowed MSD of oscillating (orange) and non-oscillating cells (blue) on Pluronic-coated, micropost arrays, and Matrigel-coated glass surfaces. (D) Real-time MSD of oscillating and non-oscillating cells on Pluronic-coated, micropost arrays, and Matrigel-coated glass surfaces.

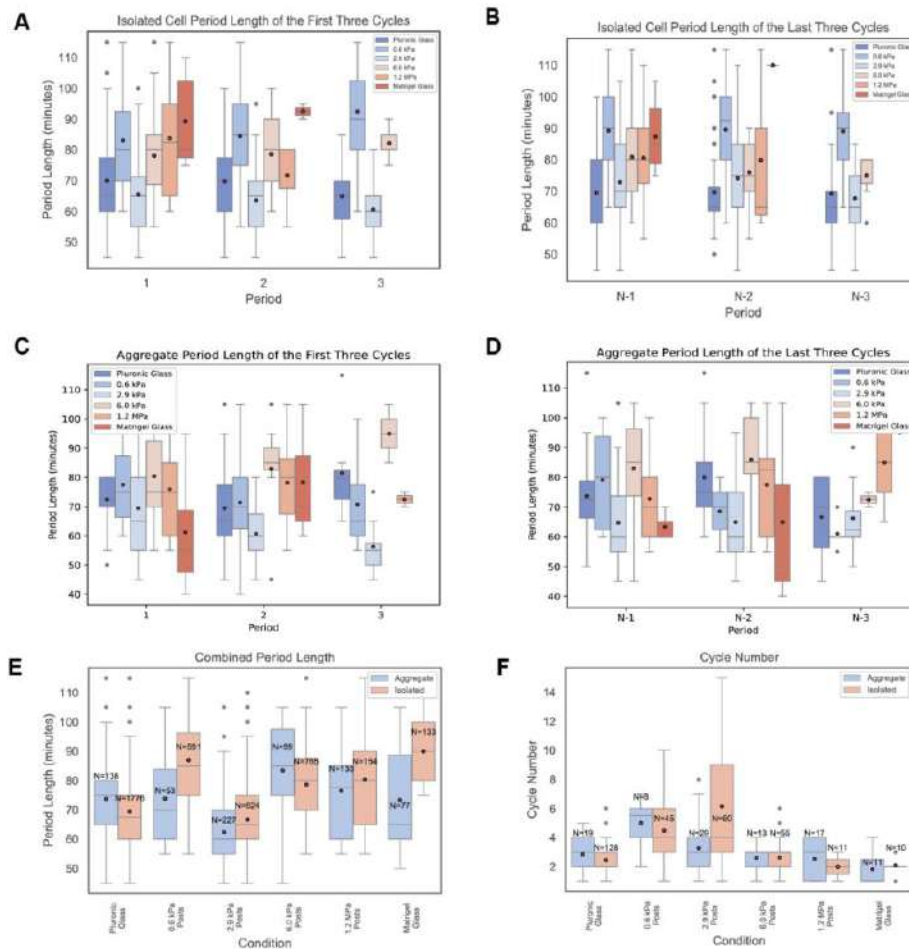


Figure S5: Comparison of oscillation period length and cycle number between isolated cells and cell aggregates.

(A, B) Period length of the first three (A) and last three (B) oscillation cycles for isolated cells cultured on surfaces of varying rigidities. The boxplots represent the distribution of period lengths, with the mean values indicated by red dots and outliers by blue dots. This analysis allows for the assessment of period length stability and variability over time in isolated cells.

(C, D) Period length of the first three (C) and last three oscillation (D) cycles for cell aggregates cultured on surfaces of varying rigidities. The boxplots follow the same conventions as in (A, B). Comparing the period lengths of isolated cells and cell aggregates provides insights into the potential influence of cell-cell interactions on the temporal dynamics of oscillations.

(E) Comparison of the overall period length between isolated cells and cell aggregates across all surface conditions. This analysis highlights any systematic differences in the oscillation period between isolated cells and cell aggregates, providing insights into the impact of cell-cell interactions on the temporal characteristics of the oscillations.

(F) Comparison of the total number of oscillation cycles between isolated cells and cell aggregates across all surface conditions. The boxplots display the distribution of cycle numbers, with mean values indicated by red dots and outliers by blue dots. This comparison reveals potential differences in the sustainability of oscillations between isolated cells and cell aggregates.

Movie S1: Isolated PSM cells on Pluronic-coated and Matrigel-coated glass conditions. Left to right: Pluronic-coated glass and Matrigel-coated glass. White arrow: oscillating cells; black arrow: non-oscillating cells. Scale bar: 50 μm .

Movie S2: Isolated PSM cells on varying rigidity conditions. White arrow: oscillating cells; black arrow: non-oscillating cells. Scale bar: 50 μm .

Movie S3: Multiple cycle traces from an oscillating cell on 2.9 kPa micropost arrays. Scale bar: 50 μm .

Movie S4A: Oscillating cell on 0.6 kPa micropost arrays. Scale bar: 10 μm .

Movie S4B: Non-oscillating cell on 0.6 kPa micropost arrays. Scale bar: 10 μm .

Movie S4C: Oscillating cell on 2.4 kPa micropost arrays. Scale bar: 10 μm .

Movie S5C: Non-oscillating cell on 2.4 kPa micropost arrays. Scale bar: 10 μm .

Movie S5A: On 2.9 kPa micropost arrays and Pluronic-coated glass. Scale bar: 50 μm .

Movie S5B: On 1.2 MPa micropost arrays. Scale bar: 50 μm . The migration of cells from the aggregate's center to its edge coincided with a loss of *Her1* oscillation and increased cellular spreading.